The Effect of Two-Photon Absorption on the Dynamic Range of Integrated Microwave Photonics Links

Jake Bass[a], Brandon Brea[b], Huong Tran[a], Wei Du[b,*], Richard Soref[c], and Shui-Qing Yu[a,*]
[a]Department of Electrical Engineering, University of Arkansas, Fayetteville, AR 72701 USA;
[b]Department of Electrical Engineering and Physics, Wilkes University, Wilkes-Barre, PA 18766 USA;
[c]Department of Engineering, University of Massachusetts Boston, Boston, MA 02125 USA

ABSTRACT

Recently, Integrated Microwave Photonics (IMWP) on Silicon-on-Insulator (SOI) platform has attracted much attention. SOI as a platform for passive devices has been studied for operation at a wavelength of 1.55 μm. It has been acknowledged that Si suffers from Two-Photon Absorption (TPA) at this wavelength, which potentially limits the dynamic range of microwave photonic links. The TPA effect diminishes at longer wavelengths, and completely vanishes at a wavelength of 2.2 μm. So far, the detailed effects of TPA on the performance of the SOI platform in the context of IMWP have not been well-explored. In this work, a systemic simulation has been performed in order to investigate the effects of nonlinear TPA on the performance of SOI microwave photonic links at 1.55 μm, particularly the dynamic range of the system was studied in-depth. Furthermore, system performance at wavelengths from 1.55 to 2.2 μm was investigated by scaling the device design, where the parasitic effects of TPA are avoided. Based on theoretical analysis, the result showing microwave photonic links at 2.2 μm outperform that at 1.55 μm was obtained as expected. Strip and rib waveguides at 1.55 μm show P1dB points of 3.75 mW and 69.54 mW, respectively, and at 2.2 μm, these waveguides performed linearly throughout the simulated range (up to 1 W of input power) which is due to the dramatically reduced TPA effect. It is noted that the wavelengths at which SOI avoids parasitic TPA match well with the working wavelengths of emerging GeSn lasers and photodetectors.

Keywords: Silicon Photonics, Integrated Microwave Photonics, Photonic Links, Two-Photon Absorption

1. INTRODUCTION

Silicon-on-Insulator (SOI) has attracted increasing attention for integrated photonics applications. SOI has found success due to its low cost, large scale on-chip integration, compatibility with current complementary metal-oxide-semiconductor (CMOS) processes. Currently, SOI is being utilized for integrated microwave photonics (IMWP) that operates at 1.55 μm. As SOI systems improve and modulators are linearized, the ever-increasing dynamic ranges (DR) for SOI integrated circuits has been achieved. Although this trend is promising for the future of SOI photonics, Si experiences parasitic two photon absorption (TPA) at 1.55 μm which will ultimately limit the DR performance on this platform. However, the impact of TPA on the DR in silicon photonics has not yet been studied in-depth. In this work, the TPA problem was investigated via numerical simulation.

The simulations in this study consider strip and rib waveguides designed for operation for wavelengths from 1.55 to 2.2 μm and for waveguide lengths from 10 to 100 mm. The results show that parasitic TPA increases as waveguide length increases, since the interaction time between the incident light and the Si is increased. Moreover, TPA has a stronger impact on strip waveguides when compared to rib waveguides. This stronger effect in strip waveguides is due to the strip design confining the incident light into a smaller effective area, increasing the intensity of light in the waveguide.

*email: syu@uark.edu; wei.du@wilkes.edu

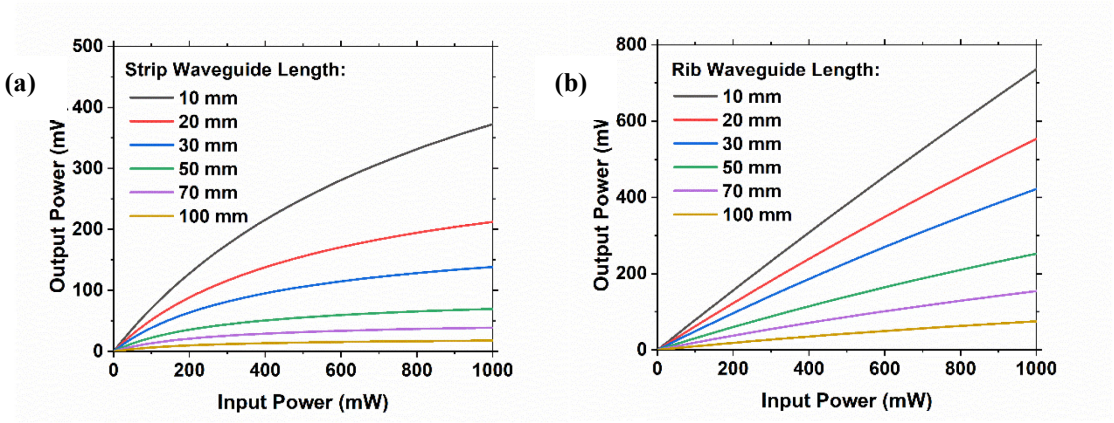

Figure 1. Power transfer characteristics for (a) a strip waveguide (left, A_{eff} = 0.19718 μm^2) and (b) a rib waveguide (right, A_{eff} = 5.1848 μm^2) operating at 1.55 μm wavelength.

2. THEORETICAL BACKGROUND

2.1 Mechanism of Two-Photon Absorption

Normally when light interacts with a material, one photon may be absorbed by an electron in the material which excites the electron to a higher energy state (one-photon absorption). Such absorption can occur only when the photon has sufficient energy to excite the electron to a certain higher energy state. In Si photonics, photons with wavelengths shorter than 1.1 μm can be absorbed.

Although a single photon at 1.55 μm is insufficient to excite the electron, the total energy of two photons at 1.55 μm has sufficient energy and could excite an electron. Therefore, if two photons at 1.55 μm interact with Silicon, there is a possibility that both photons can be simultaneously absorbed to excite one electron to a higher energy state, resulting in unwanted losses in Si based devices such as a waveguide. This mechanism is known as TPA. Since the possibility of TPA occurrence is input power dependent, at low power TPA may be considered negligible. However, as power intensity increases, TPA incidents occur more frequently, leading to significant material absorption and thus the saturation of output power as seen in Fig. 1 (a). Furthermore, the longer a waveguide length, the more incident light interactions with the Si atoms, which leads to more TPA and thus the waveguide loss increases. Therefore, TPA effects are determined principally by the waveguide length and the intensity of the light in the waveguide. Since rib waveguides distribute the light over a larger area, less TPA effects were observed in the rib design in Fig. 1 (b).

Figure 1 shows the impact of TPA on the power transfer characteristic of strip and rib waveguides operating at 1.55 μm. Although shorter waveguides are far less affected by TPA, a 10 cm long strip waveguide shows a linear operating range restricted to 3.75 mW (for 46.7 mW of input power). For the rib waveguide, a 10 cm long device shows linear operation until approximately 69.5 mW (for 902 mW of input power). It is clear that the TPA problem could significantly deteriorate the SOI photonics device performance for relative high-power applications.

2.2 Quantitative Analysis of Two-Photon Absorption

The loss introduced into a signal as a result of TPA is proportional to the square of the intensity of the light in the waveguide:[2]

$$\frac{\partial I}{\partial z} = -\beta_{TPA} I^2 \qquad (1)$$

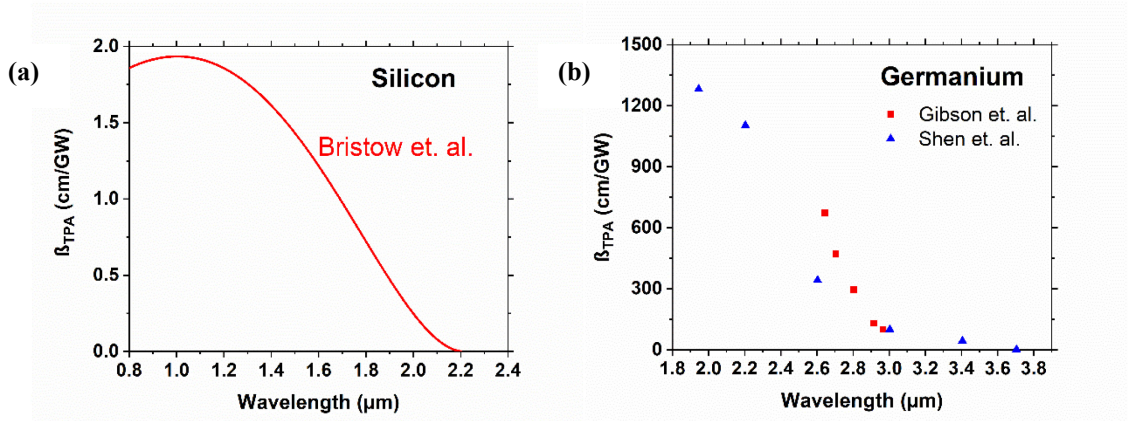

Figure 2. TPA coefficient values of (a) Silicon[3] and (b) Germanium[1,4]. The strength of the TPA effect in Ge is approximately three orders of magnitude higher than in Si.

where β_{TPA} is the two-photon absorption coefficient, I is the intensity of light in the waveguide, and z is the waveguide length. Taking the TPA effect into account and including the contribution of the linear loss in the system (i.e. the loss experienced by small-signal experiments), the complete TPA equation can be obtained as:

$$\frac{\partial I}{\partial z} = -\alpha I - \beta_{TPA} I^2 \tag{2}$$

where α is the linear loss coefficient of the waveguide. Equation (2) is relatively straightforward to solve; by introducing a substitution $u = I^{-1}$ equation (2) can be re-written as the following:

$$\frac{du}{dz} = \alpha u + \beta_{TPA} \tag{3}$$

The equation (3) can be solved by using the integrating factor method, where the integrating factor is given by

$$\mu = e^{\int -\alpha dz} = e^{-\alpha z} . \tag{4}$$

Multiplying both sides of equation (3) with the integration factor in equation (4) and integrating yields:

$$u = \frac{-I_0 \frac{\beta_{TPA}}{\alpha}(e^{-\alpha z}-1)+1}{I_0 e^{-\alpha z}} \tag{5}$$

where $I_0 = I(z = 0)$. Recovering an expression for I using $u = I^{-1}$ and simplifying gives the final result:

$$I(z) = \frac{I_0 \alpha e^{-\alpha z}}{I_0 \beta_{TPA}(1-e^{-\alpha z}) + \alpha} \tag{6}$$

Equation 6 is the result used as the foundation of all of the waveguide simulations performed in the rest of this paper. In each case, the silicon TPA coefficient values shown in Fig. 2 was used.[3] The spectral β_{TPA} and Si and Ge are plotted in Fig. 2. It is worth noting that at 2.2 μm, the TPA absorption coefficient in Si is zero, i.e., a waveguide operating at 2.2 μm could completely avoid the TPA effect.

2.3 Free-Carrier Absorption and Free-Carrier Dispersion

When a pair of photons are absorbed via TPA, a pair of carriers (electron and hole) are generated due to the excitement of an electron from the valance band to the conduction band. These unwanted carriers further degrade device performance through Free-Carrier Absorption (FCA) and Free-Carrier Dispersion (FCD). While the FCA serves to further reduce the signal carried in a waveguide experiencing TPA, the FCD introduces unwanted dispersion into the signal by locally changing the refractive index of the material where free carriers are generated[5]. These effects have been briefly studied in silicon elsewhere[2,5,6] Although free-carrier effects were not included in this study, these effects are still of interest for silicon photonics engineers and may constitute an area of further study concerning the TPA effect for MWP applications.

3. METHODOLOGY

Table 1 summarizes the structures and geometries studied in this work. These dimensions were chosen in order to ensure single-mode operation of the waveguide[7]. Single-mode operation is focused in this work, since the higher order modes would exhibit different optical properties, notably the effective index of refraction. These different optical properties would lead to undesirable effects (such as dispersion) and the different modes couple between waveguides differently, leading to complications when designing components such as Micro Ring Resonators (MRRs) which depend on waveguide-to-waveguide direction coupling.

In this work, Lumerical MODE Solutions was used. Additionally, RSoft's FullWAVE software (an FDTD simulation package) was used to recreate the waveguides and confirm parameters such as effective index and mode profile obtained from Lumerical MODE. Good agreement was found between the two simulation packages.

The spatially-dependent intensity values (measured in $\frac{W}{m^2}$) for each cell of the simulation mesh were exported in order to apply the TPA effect, since the TPA effect is nonlinear with respect to the intensity of the light. This process was repeated for waveguides that were designed for the wavelengths from 1.55 µm to 2.2 µm and the waveguide lengths from 10 to 100 mm. The intensity data was then imported into Matlab where the TPA effect was applied using the solution of equation (6) defined in the previous section. TPA coefficient β_{TPA} shown in Fig. 2 and a linear absorption coefficient value of $1\frac{dB}{cm}$ were used across each of the simulated waveguides. The distribution of intensity data points from Lumerical MODE was scaled up to simulate higher power being input to the waveguide, and the change in intensity due to the TPA equation was recorded. Finally, the post-TPA intensity values were integrated over the full area of the waveguide in order to determine the total power.

Table 1. Summary of simulated 100 mm waveguides

Waveguide Type	Wavelength (µm)	W (µm)	H (µm)	h (µm)	P1dB Point (mW)	Effective Area A_{eff} (μm^2)
Strip	1.55	0.45	0.22	N/A	3.75	0.098
Strip	1.64	0.47	0.23	N/A	4.01	0.11
Strip	1.78	0.51	0.25	N/A	6.58	0.13
Strip	1.92	0.55	0.27	N/A	13.95	0.15
Strip	2.06	0.59	0.29	N/A	51.34	0.17
Strip	2.20	0.63	0.31	N/A	N/A	0.20
Rib	1.55	1.85	2.00	1.30	69.54	5.19
Rib	1.64	1.96	2.12	1.38	76.59	5.76
Rib	1.78	2.13	2.30	1.49	124.66	6.79
Rib	1.92	2.29	2.48	1.61	N/A	7.90
Rib	2.06	2.46	2.66	1.73	N/A	9.09
Rib	2.20	2.63	2.84	1.85	N/A	10.37

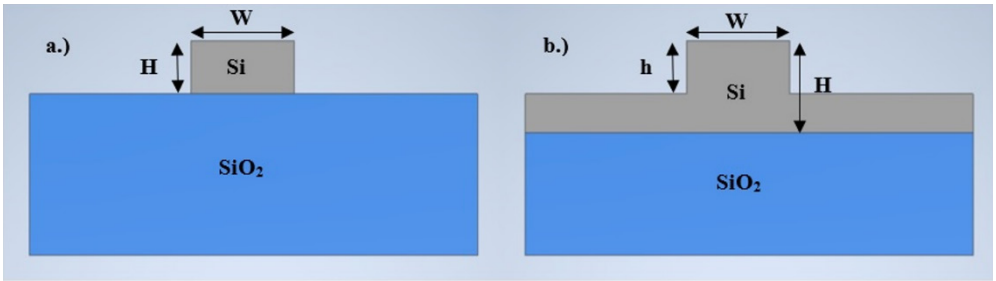

Figure 3. Schematic drawings of simulated waveguide structures for both (a) strip and (b) rib designs. Labelled height and width values correspond to values listed in Table 1.

Figure 3 shows the schematic layout of the strip and rib waveguides studied in this work. In both cases, W denotes the width of the waveguide. In the strip design, H denotes the height of the Si strip above the SiO_2 substrate. In the rib design, h denotes the height of the etched Si rib, while H denotes the total thickness of the Si layer above the SiO_2 layer. These definitions align with the W, H, and h columns presented in table 1.

4. RESULTS AND DISCUSSION

Firstly, the simulations indicate that TPA is more pronounced in strip waveguides than in rib waveguides as can be clearly seen in Fig. 4. This is an expected result since rib waveguides have a larger effective area and therefore has lower intensity when compared to the strip design carrying the same power. Furthermore, as the operating wavelength increases, the geometry of the waveguide was scaled up accordingly in order to maintain single mode operation. Specific dimensions for the simulated waveguides are provided in table 1. The scaling factor at longer wavelengths further reduced the TPA contribution by increasing the effective area, lowering light intensity in the waveguide. In order to observe the TPA effect on dynamic range, the TPA-limited linear operating range of each waveguide was determined.

Figure 4 shows the power transfer characteristics of 100 mm strip and rib waveguides operating at wavelengths from 1.55 µm to 2.2 µm. The nonlinear characteristic resulting from TPA can be clearly seen in these figures. As the optical wavelength is increased, the devices become more and more linear. At 2.2 µm, both the strip and rib waveguides operate linearly throughout the simulated range as should be expected since photons at this wavelength do not have sufficient energy to induce the TPA effect. This trend is also expected from inspection of the TPA coefficient shown in Fig. 2 (a).

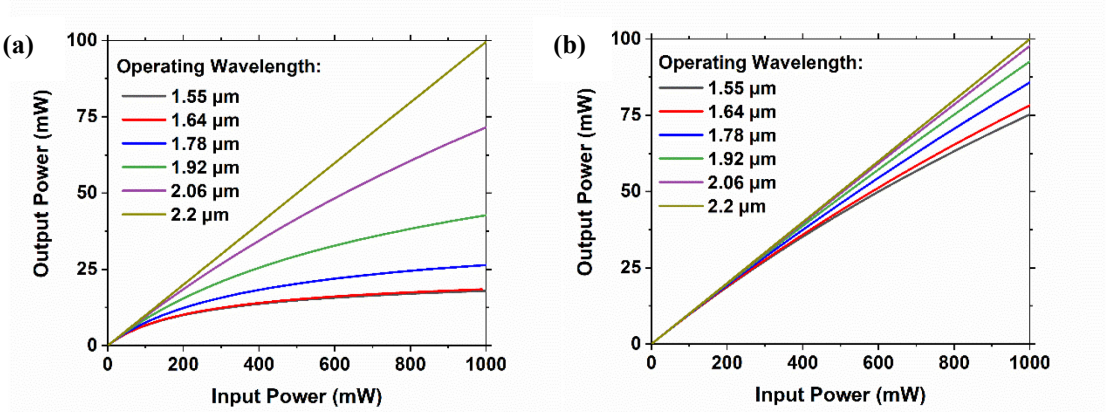

Figure 4. Power Transfer characteristics of simulated (a) strip waveguides and (b) rib waveguides. All waveguide lengths are 100 mm. Effective area and geometry characteristics are given in Table 1.

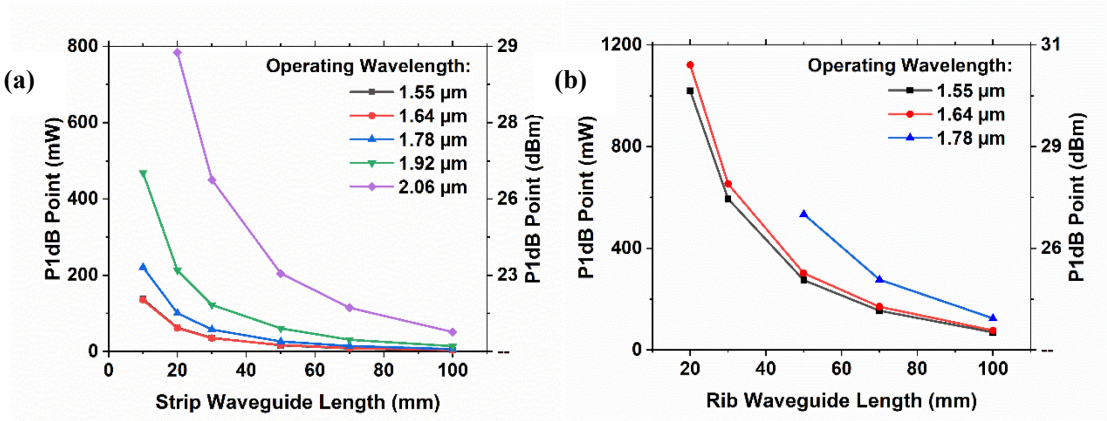

Figure 5. P1dB points as a function of waveguide length for optical wavelengths from 1.55 µm to 2.2 µm for (a) strip waveguides and (b) rib waveguides. Data points for longer wavelengths fell outside of the scope of the considered simulation range and thus were not included in this analysis.

One figure-of-merit applied to components of MWP circuits is the P1dB point, which determines the linear operating regime of that component. The P1dB point is defined as the output power at which the loss of the component reduces to 1 dB below the input power, when distortion effects become impermissible to be used in practical designs. The P1dB point restricts the dynamic range as a function of bandwidth B and total output noise power spectral density N_{out} given by:[8]

$$\mathrm{CDR_{1dB}} = \frac{P_{1dB}10^{1/10}}{N_{out}B} \tag{7}$$

The P1dB point was calculated for a wide range of waveguide lengths and optical wavelengths for both strip and rib waveguide designs, and those results are shown in Fig. 5. Although the spurious-free dynamic range (SFDR) of current IMWP systems are below the Compression Dynamic Range (CDR) imposed by the waveguides, as modulators are improved and SFDR is increased, eventually the limiting factor for the dynamic range of photonic circuits will no longer be the SFDR of the modulator, but rather the CDR of the waveguides themselves.

Furthermore, TPA presents a more insidious danger to engineers designing IMWP circuits. Although one may find reported in the literature the dynamic range of some component, that component was likely tested using a photonic circuit of some very short length, as it would only contain the component under test. When a practical circuit is designed, where many functionalities are required, the total circuit length can become much longer, leading to a device with a practical dynamic range much lower than expected, and this reduced dynamic range would only be discovered after the entire circuit has been fabricated unless the designer has already considered how TPA would limit the dynamic range. However, as mentioned previously, if the optical wavelength of the light used in an SOI circuit is greater than 2.2 µm, then TPA can be avoided completely, and so TPA-induced compression will not reduce the dynamic range of IMWP devices even at high input power.

4.1 Further Discussion

As the state-of-the-art progresses, these results suggest MWP systems utilizing the strip waveguide design will be the first to observe TPA-limited dynamic ranges, followed by those using the rib design. However, if the operating wavelength used by MWP systems migrates from 1.55 µm to beyond 2.2 µm, the TPA problem can be avoided completely.

It should be noted that researchers have found some useful applications for the TPA effect, such as for designing an all-optical modulator[1] or optical logic gates.[2] If a circuit designer seeks to leverage TPA for applications such as these, they should find success using Ge rather than Si, since Ge exhibits a TPA coefficient approximately 1000X stronger than that of Si, as can be seen in Fig. 2.

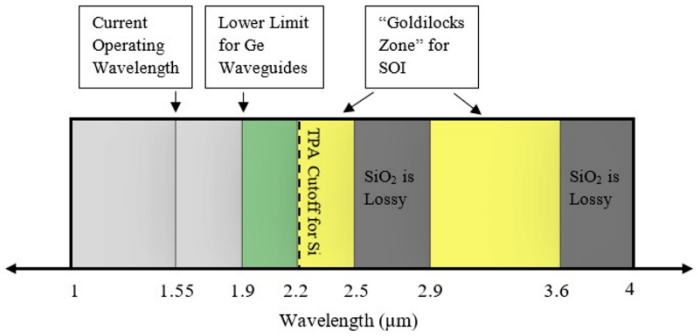

Figure 6. Diagram outlining some of the advantages of the "Goldilocks Zone" operating wavelength range for SOI.

Figure 6 shows that there exists a "Goldilocks Zone" for SOI where, on the one hand the operating wavelength is high enough to avoid parasitic TPA and, on the other hand the wavelength is not so high such that the SiO_2 insulator becomes lossy. Furthermore, the Goldilocks Zone has the added advantage of being able to leverage Germanium-on-Silicon components, which can take advantage of some of Germanium's optical properties such as its nonlinear response which is much stronger when compared to Silicon. It should be noted that low-loss Silicon waveguides have already been demonstrated in the Goldilocks Zone.[9,10]

Since the SOI platform has been developed for operation at 1.55 μm, there may be concern that by migrating to the Goldilocks Zone beyond 2.2 μm there will be a lack of materials to be used for active devices for both integration and testing purposes. One candidate for active devices in the Goldilocks Zone is found in the Group IV SiGeSn material system. The SiGeSn system theoretically allows for arbitrary compositions of Silicon, Germanium, and Tin. The possibility for arbitrary compositions means SiGeSn constitutes a flexible material system with both indirect bandgap and direct bandgap capabilities which can be tuned to cover the entire Goldilocks Zone. These capabilities along with the fact that chemical vapor deposition growth of GeSn is a low-cost, low-temperature process suggest that the SiGeSn system may be the optimal material for both on-chip and off-chip active devices.[11,12]

5. CONCLUSIONS

These simulation results suggest that the dynamic range of MWP systems will be limited by TPA as these systems are equipped to handle high-power signals. For the waveguide designs considered in this study, the linear operating range of waveguides defined by the P1dB point are limited to 46.7 mW and 902 mW of input power for 100 mm strip and rib waveguides operating at 1.55 μm, respectively. Due to the FCA effect, which was not considered in these simulations, it is expected that experimental results will demonstrate linear operating ranges which are even more restricted by TPA, particularly for waveguides demonstrating lower linear loss characteristics.

Development of group IV active devices to cover the Goldilocks Zone is already under way. GeSn electrically injected light emission has already been demonstrated on the SOI platform.[13] Near-room temperature (270K) optically pumped lasing has also been demonstrated using the SiGeSn material system using waveguide lasing structures designed with Si photonics integration in mind.[14,15] Furthermore, high-speed photodetection utilizing a GeSn/Ge multiple quantum well (MQW) photodiode has already been demonstrated on Si substrate at 2 μm operation,[16] and GeSn/Ge MQW photodetectors have been demonstrated which cover the 2.2 μm to 2.5 μm Goldilocks window with less than 10% Sn incorporation required.[17] These recent results suggest that the group IV material system is a promising candidate for developing active devices on SOI operating beyond 2.2 μm, where the TPA problem can be avoided completely.

ACKNOWLEDGEMENTS

The authors would like to acknowledge financial support from the Air Force Office of Scientific Research (AFOSR) (Grant No. FA9550-18-1-0361) and the National Science Foundation (Grant No. ECCS-1745143) which has enabled this research. Dr. Wei Du also appreciates support from Provost's Research & Scholarship Fund at Wilkes University.

REFERENCES

[1] Shen, L., Healy, N., Mitchell, C. J., Pernades, J. S., Nedeljkovic, M., Mashanovich, G. Z. and Peacock, A. C., "Two-photon absorption and all-optical modulation in germanium-on-silicon waveguides for the mid-infrared," Opt. Lett. Vol. 40, No. 10, (2015).

[2] Choudhury, R. V. R., "FCA based Two Photon Absorption and Simulation of Si Waveguide to device Optical Logic Gates," IEEE Worksh. Rec. Adv. Phot., (2015).

[3] Bristow, A. D., Rotenberg, N. and van Driel, H. M., "Two-photon absorption and Kerr coefficients of silicon for 850 – 2200 nm," Appl. Physl Lett. 90, 191104 (2007).

[4] Gibson, A. F., Hatch, C. B., Maggs, P. N. D., Tilley, D. R. and Walker, A. C., "Two-photon absorption in indium antimonide and germanium," J. Phys. C 9, 3259 (1976).

[5] Yin, L. and Agrawal, G. P., "Impact of two-photon absorption on self-phase modulation in silicon waveguides," Opt. Lett. Vol. 32, No. 14, (2007).

[6] Suzuki, N., "FDTD Analysis of Two-Photon Absorption and Free-Carrier Absorption in Si High-Index-Contrast Waveguides," J. Light. Tech. Vol. 25, No. 9, (2007).

[7] Huang. H., Liu, K., Qu, B. and Sorger, V. J., "Re-analysis of single-mode conditions for Silicon rib waveguides at 1550 nm wavelength," J. Light. Tech. Vol. 34, No. 16, (2016).

[8] Urick Jr., V. J., McKinney, J. D. and Williams, K. J., [Fundamentals of Microwave Photonics], John Wiley & Sons, Inc., Hoboken, New Jersey, 33-56, (2015).

[9] Mashanovich, G. Z., Milosevic, M. M., Nedeljkovic, M., Owens, N., Xiong, B., Teo, E. J. and Hu, Y., "Low loss silicon waveguides for the mid-infrared," Opt. Exp., Vol. 19, No. 8 (2011).

[10] Milosevic, M. M., Matavulj, P. S., Yang, P. Y., Bagolini, A. and Mashanovich, G. Z., "Rib waveguides for mid-infrared silicon photonics," J. Opt. Soc. Am. Vol. 26, No. 9, (2009).

[11] Ghetmiri, S. A., Tran, H., Mosleh, A., Du, W., Liu, J., Li, B., Mortazavi, M. and Yu, S. Q., "Si-Based GeSn Photodetector for Mid-Infrared Integrated Microwave Photonics,"

[12] Grant, P. C., Dou, W., Alharthi, B., Grant, J. M, Tran, H., Abernathy, G., Mosleh, A., Du, W., Li., B., Mortazavi, M., Naseem, H. A. and Yu, S. Q., "UHV-CVD growth of high quality GeSn using $SnCl_4$: from material growth development to prototype devices," Opt. Mat. Exp. Vol. 9, No. 8, (2019).

[13] Huang, B. J., Chang, C. Y., Hsieh, Y. D., Soref, R. A., Sun, G., Cheng, H. H. and Chang, G. E., "Electrically Injected GeSn Vertical-Cavity Surface Emitters on Silicon-on-Insulator Platforms," ACS Photonics 6, 1931-1938, (2019).

[14] Zhou, Y., Dou, W., Du, W., Ojo, S., Tran, H., Ghetmiri, S. A., Liu, J., Sun, G., Soref, R., Margetis, J., Tolle, J., Li, B., Chen, Z., Mortazavi, M., and Yu, S. Q., "Optically Pumped GeSn Lasers Operating at 270 K with Broad Waveguide Structures on Si," ACS Photonics 6, 1434-1441, (2019).

[15] Zhou, Y., Margetis, J., Abernathy, G., Dou, W., Grant, P. C., Alharthi, B., Du, W., Wadsworth, A., Guo, Q., Tran, H., Ojo, S., Mosleh, A., Getmiri, S. A., Thompson, G. B., Liu, J., Sun, G., Soref, R., Tolle, J., Li, B., Mortazavi, M. and Yu, S. Q., "Investigation of SiGeSn/GeSn/SiGeSn Quantum Well Structures and Optically Pumped Lasers on Si," CLEO, (2019)

[16] Xu, S., Wang, W., Huang, Y. C., Dong, Y., Masudy-Panah, S., Wang, H., Gong, X. and Yeo, Y. C., "High-speed photo detection at two-micron-wavelength: technology enablement by GeSn/Ge multiple-quantum-well photodiode on 300 mm Si substrate," Opt. Exp. Vol. 27, No. 4, (2019).

[17] Tran, H., Littlejohns, C. G., Thomson, D. J., Pham, T., Ghetmiri, A., Mosleh, A., Margetis, J., Tolle, J., Mashanovich, G. Z., Du, W., Li, B., Mortazavi, M. and Yu, S. Q., "Study of GeSn Mid-Infrared Photodetectors for High Frequency Applications," Frontiers in Materials, Vol. G, Art. 278, (2019).